

Imprints of CP-violating phases induced by sterile neutrinos in T2K

N. Klop* and A. Palazzo

Max-Planck-Institut für Physik (Werner Heisenberg Institut), Föhringer Ring 6, 80805 München, Germany

We investigate the impact of light (\sim eV) sterile neutrinos in the long-baseline experiment T2K. We show that, within the 3+1 scheme, for mass-mixing parameters suggested by the short-baseline anomalies, the interference among the sterile and the atmospheric oscillation frequencies induces a new term in the $\nu_\mu \rightarrow \nu_e$ transition probability, which has the same order of magnitude of the standard 3-flavor solar-atmospheric interference term. We find that current T2K data, taken together with the results of the θ_{13} -dedicated reactor experiments, are sensitive to two of the three CP-violating phases involved in the 3+1 scheme. Both the standard CP-phase and the new one ($\delta \equiv \delta_{13}$ and δ_{14} in our parameterization choice) tend to have a common best fit value $\delta_{13} \simeq \delta_{14} \simeq -\pi/2$. Quite intriguingly, the inclusion of sterile neutrino effects leads to a better agreement among the two estimates of θ_{13} obtained, respectively, from reactors and T2K, which in the 3-flavor framework are slightly different.

PACS numbers: 14.60.Pq, 14.60.St

I. INTRODUCTION

Neutrino physics is entering a new era. The discovery of a relatively large value of the long-sought third mixing angle θ_{13} has raised hopes of completing the picture of the standard 3-flavor framework. The determination of the two missing unknown properties, i.e., the amount (if any) of leptonic CP-violation (CPV) and the neutrino mass hierarchy (NMH) are now realistic targets.

CPV is a genuine 3-flavor phenomenon [1], which can occur only if no pair of neutrino mass eigenstates is degenerate ($m_i^2 - m_j^2 \neq 0$ for $i \neq j$, $i, j = 1, 2, 3$) and if all the three mixing angles ($\theta_{12}, \theta_{23}, \theta_{13}$) are non-zero. Now that all these (six) necessary conditions are known to be realized in Nature, the next task is to ascertain if a further (last) condition is fulfilled, i.e. if the lepton mixing matrix is non-real, or equivalently if the CP-phase δ is different from 0 and π . The CP-phase δ is already being probed by the long-baseline (LBL) accelerator experiment T2K [2] (and also by MINOS [3] with less statistical power) in combination with the reactor θ_{13} -dedicated experiments [4–7], which “fix” θ_{13} independently of δ . Some (weaker) information on such a fundamental phase is also provided by atmospheric neutrinos [8]. Quite intriguingly, all the latest global analyses [9–11] show a weak indication (close to the 90% C.L.) of CPV, the best fit value of the CP-phase being $\delta \sim -\pi/2$.

An apparently unrelated issue in present-day neutrino physics is provided by the hints of light (\sim eV) sterile species suggested by the short-baseline (SBL) anomalies (see [12–14] for reviews). In the presence of sterile neutrinos, the 3-flavor scheme must be enlarged so as to include one (or more) mass eigenstates having non-zero admixture with the active flavors. In such more general frameworks, new CP-phases automatically appear and

thus the question naturally arises as to whether the current and planned LBL experiments, designed to underpin the standard CP-phase δ , have also some chance to detect the new potential sources of CPV.¹

In this work we show that the existing measurements of $\nu_\mu \rightarrow \nu_e$ appearance performed by the LBL experiment T2K, taken in combination with those of $\bar{\nu}_e \rightarrow \bar{\nu}_e$ disappearance deriving from the θ_{13} -dedicated reactor experiments, are *already* able to provide information on the non-standard sterile-induced CP-phases. In fact, differently from the SBL experiments, in LBL setups the oscillations induced by the new sterile neutrino species can interfere with those driven by the two standard squared-mass splittings giving rise to observable effects. In particular, it turns out that the interference among the sterile and the atmospheric oscillation frequencies induces a new term in the $\nu_\mu \rightarrow \nu_e$ transition probability, which has the same order of magnitude of the standard 3-flavor solar-atmospheric interference term.

Working within the simple 3+1 scheme, we show that, for mass-mixing parameters suggested by the current SBL fits [13, 14], it is possible to extract quantitative information on two of the three CP-phases involved in the model (one of them being the standard phase δ). Quite intriguingly, the statistical significance of the information obtained on the new CP-phase is similar to that achieved for the standard phase δ . In addition, our analysis evidences that the presence of 4-flavor effects tends to resolve the slight tension (present within the 3-flavor framework) between the two estimates of θ_{13} extracted, respectively, from T2K and from reactors experiments.

The rest of the paper is organized as follows. In Sec. II we introduce the theoretical framework needed to discuss the analytical behavior of the LBL $\nu_\mu \rightarrow \nu_e$ transition probability in vacuum. In Sec. III we present the results

*Now at GRAPPA Institute, University of Amsterdam, Science Park 904, 1098 XH Amsterdam, Netherlands

¹ Previous work on the effects of light sterile neutrinos in LBL setups can be found in [15–24].

of the numerical analysis (which includes the matter effects). In Sec. III we draw our conclusions. The paper is closed by an Appendix dedicated to the analytical treatment of the MSW effects relevant for the LBL setups within the 3+1 scheme.

II. THEORETICAL FRAMEWORK

Light sterile neutrinos are introduced in the so-called $3 + N_s$ schemes, where the N_s new mass eigenstates are assumed to be separated from the three standard ones by large splittings, giving rise to the hierarchal pattern $\Delta m_{12}^2 \ll |\Delta m_{13}^2| \ll |\Delta m_{1k}^2|$ ($k = 4, \dots, 3 + N_s$), where $\Delta m_{ij}^2 \equiv m_j^2 - m_i^2$. This implies that the fast oscillations induced by the new squared-mass splittings are completely averaged in all setups sensitive to the solar squared-mass difference (Δm_{12}^2) and the atmospheric one (Δm_{13}^2). In this work, for definiteness, we consider the simplest 3+1 scheme.

In the presence of a fourth sterile neutrino ν_s , the flavor (ν_α , $\alpha = e, \mu, \tau, s$) and the mass eigenstates (ν_i , $i = 1, 2, 3, 4$), are connected through a 4×4 unitary mixing matrix U , which depends on six complex parameters [25]. Such a matrix can be expressed as the product of six complex elementary rotations, which define six real mixing angles and six CP-violating phases. Of the six phases three are of the Majorana type and are unobservable in oscillation processes, while the three remaining ones are of the Dirac type. As it will appear clear in what follows, for the treatment of the transitions involved in LBL setups, a particular convenient choice of the parameterization of the mixing matrix is

$$U = \tilde{R}_{34} R_{24} \tilde{R}_{14} R_{23} \tilde{R}_{13} R_{12} \quad (1)$$

where R_{ij} (\tilde{R}_{ij}) represents a real (complex) 4×4 rotation in the (i, j) plane containing the 2×2 submatrix

$$R_{ij}^{2 \times 2} = \begin{pmatrix} c_{ij} & s_{ij} \\ -s_{ij} & c_{ij} \end{pmatrix} \quad \tilde{R}_{ij}^{2 \times 2} = \begin{pmatrix} c_{ij} & \tilde{s}_{ij} \\ -\tilde{s}_{ij}^* & c_{ij} \end{pmatrix}, \quad (2)$$

in the (i, j) subblock, with

$$c_{ij} \equiv \cos \theta_{ij} \quad s_{ij} \equiv \sin \theta_{ij} \quad \tilde{s}_{ij} \equiv s_{ij} e^{-i\delta_{ij}}. \quad (3)$$

The parameterization in Eq. (1) has the following properties: I) For vanishing mixing involving the fourth state ($\theta_{14} = \theta_{24} = \theta_{34} = 0$) it reduces to the 3-flavor mixing matrix in its standard parameterization [26] with the identification $\delta_{13} \equiv \delta$; II) The leftmost positioning of the matrix \tilde{R}_{34} allows us to eliminate the mixing angle θ_{34} (and the related CP-phase δ_{34}) from the expression of the $\nu_\mu \rightarrow \nu_e$ conversion probability in vacuum. In matter, the transition probability depends also on θ_{34} and δ_{34} . However, the sterile-induced matter perturbations are extremely small in T2K and such dependency is completely negligible (see the Appendix). III) For small values of θ_{13} and of the mixing angles involving the fourth

mass eigenstate, one has $|U_{e3}|^2 \simeq s_{13}^2$, $|U_{e4}|^2 = s_{14}^2$ (exact), $|U_{\mu 4}|^2 \simeq s_{24}^2$ and $|U_{\tau 4}|^2 \simeq s_{34}^2$, with a clear physical interpretation of the new mixing angles.

Before considering the 4-flavor transition probability relevant for T2K, we recall a basic property of the 3-neutrino framework, which will be helpful in understanding the more general 4-neutrino case. In the presence of CPV, at LBL experiments one expects a non-zero value of the asymmetry

$$A_{\mu e}^{\text{CP}} \equiv P(\nu_\mu \rightarrow \nu_e) - P(\bar{\nu}_\mu \rightarrow \bar{\nu}_e), \quad (4)$$

which, in the 3-flavor (vacuum) case can be expressed as

$$A_{\mu e}^{\text{CP}} = 16 J \sin \Delta_{12} \sin \Delta_{23} \sin \Delta_{31}, \quad (5)$$

where $\Delta_{ij} \equiv \Delta m_{ij}^2 L / 4E$ (L being the baseline and E the neutrino energy) and J is the Jarlskog invariant [27]

$$J = \text{Im}[U_{e2} U_{\mu 3} U_{e3}^* U_{\mu 2}^*]. \quad (6)$$

The mass pattern chosen by Nature for the three mass eigenstates is such that in the LBL setups we have $\Delta = |\Delta_{13}| \simeq |\Delta_{32}| \sim O(1)$ and $\Delta_{12} = \alpha \Delta$, with $\alpha \simeq 0.03$. Consider, however, an ideal case where in the same setups we have $\Delta \equiv |\Delta_{13}| \simeq |\Delta_{32}| \gg 1$, while leaving Δ_{12} unaltered (this would correspond to a much larger value of $|\Delta m_{13}^2|$). In this situation, the average over the finite energy resolution of the experiment would wash out the fast oscillating terms in Eq. (5), giving rise to

$$-\langle \sin \Delta_{23} \sin \Delta_{31} \rangle \simeq \langle \sin^2 \Delta \rangle = 1/2, \quad (7)$$

thus obtaining for the CP asymmetry

$$\langle A_{\mu e}^{\text{CP}} \rangle = -8 J \sin \Delta_{12}. \quad (8)$$

This ideal case shows that CPV is not erased by the average over the two large frequencies. CPV cancellation would occur only if also the third frequency were very large ($\Delta_{12} \gg 1$). Consider now a realistic 3+1 scheme. In this case, the oscillations induced by the three new large oscillation frequencies $|\Delta_{new}| \equiv |\Delta_{14}| \simeq |\Delta_{24}| \simeq |\Delta_{34}| \gg 1$ will get averaged, and the information on their values will be lost. On the other hand, CPV effects will survive, since there are other two finite frequencies, the atmospheric [$\Delta \equiv |\Delta_{13}| \simeq |\Delta_{32}| \sim O(1)$] and the solar one ($\Delta_{12} = \alpha \Delta$). Therefore, it will be natural to expect a dependency on the CP-phases in the flavor conversion process.

Let us now come to the expression of the $\nu_\mu \rightarrow \nu_e$ transition probability probed in T2K. We recall that in the 3-flavor vacuum case, such a probability can be written as the sum of three terms

$$P_{\mu e}^{3\nu} = P^{\text{ATM}} + P^{\text{SOL}} + P^{\text{INT}}, \quad (9)$$

where the first two ones are positive definite probabilities induced by the atmospheric and the solar squared-mass splitting, while the third is an interference term, which

can assume both positive and negative values. An expansion in the small parameters $s_{13} \simeq 0.15$ and $\alpha \simeq 0.03$ (supposed to have the same order ϵ) provides, at the second order in ϵ , the well know expressions [28]

$$P_{3\nu}^{\text{ATM}} \simeq 4s_{23}^2 s_{13}^2 \sin^2 \Delta, \quad (10)$$

$$P_{3\nu}^{\text{SOL}} \simeq 4c_{12}^2 c_{23}^2 s_{12}^2 (\alpha \Delta)^2, \quad (11)$$

$$P_{3\nu}^{\text{INT}} \simeq 8s_{13}s_{12}c_{12}s_{23}c_{23}(\alpha\Delta) \sin \Delta \cos(\Delta + \delta_{13}). \quad (12)$$

While all these three terms are formally of the same (second) order in ϵ , they have quite different sizes, since α is much smaller than s_{13} . Around the first oscillation maximum ($\Delta \sim \pi/2$) probed by T2K, the atmospheric term is $\sim 5 \times 10^{-2}$, the interference term is $\sim 1.3 \times 10^{-2}$, and the solar term is $\sim 1.5 \times 10^{-3}$. Indeed, a different kind of expansion, considering $s_{13} \sim \epsilon$ and $\alpha \sim \epsilon^2$, is more appropriate, as already evidenced in [29]. In this case, an expansion at the third order gives only the (leading) atmospheric term ($\sim \epsilon^2$) and the (subleading) interference term ($\sim \epsilon^3$). A fourth order expansion returns the solar term $\propto (\alpha\Delta)^2$ of Eq. (11), and two additional terms [29]. The first of them can be interpreted as a tiny modification of the atmospheric term $\delta P^{\text{ATM}} \propto s_{13}^4$, while the second one as a very small change of the interference term $\delta P^{\text{INT}} \propto s_{13}^2(\alpha\Delta)$. All the three fourth-order terms, for the T2K baseline, have size $\lesssim 2 \times 10^{-3}$ and have negligible impact.

The analyses of the SBL anomalies [13, 14] indicate values of s_{14} and s_{24} which have sizes very similar to s_{13} . Hence, for the purposes of this work, which is limited to the SBL preferred region, it is meaningful to assume all these parameters having the same common order ϵ while considering $\alpha \sim \epsilon^2$. After averaging over the fast oscillations induced by the large frequency Δ_{14} , at the fourth-order in ϵ , we find

$$\begin{aligned} P_{\mu e}^{4\nu} \simeq & (1 - s_{14}^2 - s_{24}^2)P_{\mu e}^{3\nu} \\ & + 4s_{14}s_{24}s_{13}s_{23} \sin \Delta \sin(\Delta + \delta_{13} - \delta_{14}) \\ & - 4s_{14}s_{24}c_{23}s_{12}c_{12}(\alpha\Delta) \sin \delta_{14} \\ & + 2s_{14}^2 s_{24}^2. \end{aligned} \quad (13)$$

The first term is just the 3-flavor probability multiplied by the suppression factor $f = 1 - O(\epsilon^2)$. The second and third terms can be ascribed, respectively, to the interference of the atmospheric and solar frequencies with the new large frequency, which does not appear in the formulae since it has been averaged out. The last term can be interpreted as the averaged transition probability in an effective 2-flavor description. As it might have been expected, the transition probability is the sum of six contributions

$$\begin{aligned} P_{\mu e}^{4\nu} = & P^{\text{ATM}} + P^{\text{SOL}} + P^{\text{STR}} \\ & + P_{\text{I}}^{\text{INT}} + P_{\text{II}}^{\text{INT}} + P_{\text{III}}^{\text{INT}}. \end{aligned} \quad (14)$$

The first two terms and the fourth one coincide (apart from the suppression factor f) with the three standard

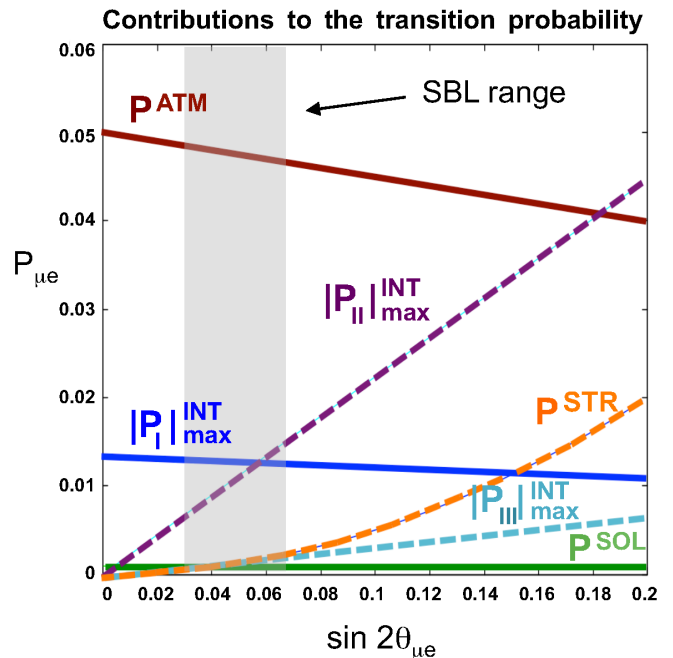


FIG. 1: Behavior of the six contributions of the transition probability as a function of the effective appearance mixing angle $\sin 2\theta_{\mu e}$ in the case $s_{14} = s_{24}$. For the three interference terms the maximum absolute value is plotted.

3-flavor terms in Eqs. (10-12). With P^{STR} we have indicated the last term in (13). The last two contributions are the new interference terms [second and third terms in Eq. (13)]. Inspection of Eq. (13) reveals that $P_{\text{II}}^{\text{INT}}$ is $O(\epsilon^3)$ so its size is expected to be comparable to that of the standard interference term $P_{\text{I}}^{\text{INT}}$. Both P^{STR} and $P_{\text{III}}^{\text{INT}}$ are $O(\epsilon^4)$ like P^{SOL} .

Let us come back for a moment to Eq. (13). From this expression we can observe that the last three terms depend on the product $s_{14}s_{24}$, and therefore they depend on the effective appearance mixing angle, defined as

$$\sin 2\theta_{\mu e} \equiv 2|U_{e4}||U_{\mu 4}| \simeq 2s_{14}s_{24}, \quad (15)$$

which is the amplitude probed in the SBL $\nu_{\mu} \rightarrow \nu_e$ experiments. The first term in Eq. (13) depends on a different combination of the two mixing angles. However, in the particular case $s_{14}^2 = s_{24}^2$, this combination can be expressed as

$$s_{14}^2 + s_{24}^2 = 2s_{14}^2 = 2s_{14}s_{24} = \sin 2\theta_{\mu e}, \quad (16)$$

and the suppression factor f as²

$$f = 1 - \sin 2\theta_{\mu e}. \quad (17)$$

² It is useful to observe that for a fixed value of the appearance angle $\sin 2\theta_{\mu e}$, the suppression factor f is always smaller than the one obtained in the specific case $s_{14}^2 = s_{24}^2$. In fact, the inequality $(s_{14} - s_{24})^2 \geq 0$ implies that $s_{14}^2 + s_{24}^2 \geq 2s_{14}s_{24} = \sin 2\theta_{\mu e}$.

Therefore, Eq. (13) can be recast in the form

$$\begin{aligned}
P_{\mu e}^{4\nu} &= (1 - \sin 2\theta_{\mu e})P_{\mu e}^{3\nu} \\
&+ 2 \sin 2\theta_{\mu e} s_{13} s_{23} \sin \Delta \sin(\Delta + \delta_{13} - \delta_{14}) \\
&- 2 \sin 2\theta_{\mu e} c_{23} s_{12} c_{12}(\alpha\Delta) \sin \delta_{14} \\
&+ \frac{1}{2} \sin^2 2\theta_{\mu e},
\end{aligned}
\tag{18}$$

in which all the terms [and consequently all the six terms in Eq. (14)] scale with a definite power of the effective appearance mixing angle.

Figure 1 displays all the six contributions in Eq. (14) as a function of $\sin 2\theta_{\mu e}$. For the three interference terms (which can be positive or negative) we plot the maximum absolute value. The vertical gray band indicates the range allowed by the SBL anomalies. As expected from the discussion made above, in this range, only the leading atmospheric and two subleading interference terms are relevant, and the 4-flavor transition probability is approximately given by

$$P_{\mu e}^{4\nu} \simeq P^{\text{ATM}} + P_{\text{I}}^{\text{INT}} + P_{\text{II}}^{\text{INT}}. \tag{19}$$

Remarkably, the amplitude of the new (atmospheric-sterile) interference term is almost identical to that of the standard (solar-atmospheric) interference term. As a consequence, a big impact on the regions reconstructed by the experiment T2K for the CP-phase δ_{13} is expected. More importantly, a similar sensitivity to the two CP-phases δ_{13} and δ_{14} is expected in the combination of T2K with the reactor experiments. The quantitative verification of these qualitative expectations will be the subject of the next section.

III. NUMERICAL ANALYSIS

In our numerical analysis we include the reactor experiments Daya-Bay and RENO and the LBL experiment T2K. Concerning T2K the analysis is slightly different for the two cases of three and four flavors, since in this last case there are appreciable oscillation effects not only at the far detector (Super-Kamiokande) but also at the near detector (ND280), which must be taken into account. For this reason, we discuss the two cases separately. In the calculation of the oscillation probability we have included the MSW effects following the prescriptions described in the Appendix.

A. Treatment of the reactor experiments

The analysis of the reactor experiments is performed using the total rate information and following the approach described in detail in [30]. For both experiments we have used the latest data presented at the Neutrino 2014 Conference [4, 7] based, respectively, on 621 live days (Daya Bay) and 800 live days (RENO). Since

the electron anti-neutrino survival probability probed by these experiments is independent of the CP-violating phases (standard and non-standard), their estimate of θ_{13} does not depend on their values. We recall that such an estimate is extracted using the ratio of the event rates measured at the far and at the near sites. Since the fast oscillations induced by Δm_{14}^2 are averaged out at both detector sites, Daya Bay and RENO are not sensitive to 4-flavor effects. As a result, their estimate of θ_{13} is independent of the mixing angle θ_{14} as far as it is allowed to vary in the range we are exploring.³ Finally, the estimate of θ_{13} is essentially identical for the two cases of normal hierarchy (NH) and inverted hierarchy (IH).

B. Treatment of T2K

1. The 3-flavor case

We use the T2K results of the $\nu_{\mu} \rightarrow \nu_e$ appearance searches [2], which reported 28 events with an estimated background of 4.92 events. In order to calculate the theoretical expectation for the total number of events and their binned spectrum in the reconstructed neutrino energy, we convolve the product of the ν_{μ} flux [31] (tables provided on the T2K home page [32]), the charged current quasi elastic (CCQE) cross-section (estimated from [2]), and the $\nu_{\mu} \rightarrow \nu_e$ transition probability, with an appropriate energy resolution function, which incorporates the correlation among the true and the reconstructed neutrino energy. We have checked that our prediction for the binned spectrum of events is in very good agreement with that shown by the collaboration in [2]. We have performed the analysis both using the total rate information and the full spectrum, observing very small differences among the two cases. This is due to the limited statistics currently available, and to the effect of the smearing induced by the energy resolution. As explained in the next subsection, in the 4-flavor case we could consistently perform only a total rate analysis. Therefore, for homogeneity, in the 3-flavor case, we report the results obtained with the total rate information.

2. The 4-flavor case

In the case of 4-flavor oscillations the T2K near detector (ND) is sensitive to the oscillations induced by the new Δm_{14}^2 , since at the baseline $L^{\text{ND}} = 280$ m, $\Delta_{14}^{\text{ND}} \sim O(1)$. To this regard, it should be noted that the published neutrino fluxes $\phi_{\nu}(E)$ (both those relative to ND280 and their extrapolations at Super-Kamiokande)

³ It can be shown that corrections to this approximation arise at the order ϵ^6 , being proportional to $s_{13}^2 s_{14}^4$, and are completely negligible.

are constrained with the measurements performed at the ND (see [31]). More precisely, the available fluxes are not the original output of the dedicated simulation programs, but are a “post-fit” version of these. Basically, the fluxes are anchored to the ND measurements, compatibly with the pulls of the nuisance parameters of the model of the original (“pre-fit”) fluxes. The anchoring of the fluxes to the ND measurements introduces an overall normalization factor and appreciable energy distortions, whose typical size is $\sim 10\%$. These effects can be appreciated for example in Fig. 1 of [2].

This procedure is designed for the 3-flavor case, in which the oscillation effects at the ND are negligible and, in this case, it improves the estimate of the non-oscillated fluxes. Differently, in the presence of 4-flavor effects, the available “post-fit” fluxes are no more an accurate estimate of the non-oscillated fluxes, since they partially incorporate the effects of the 4-flavor oscillations occurred at the ND. In the range of the small mixing angles we are exploring in this work, at the ND it is expected an energy dependent suppression of the non-oscillated fluxes whose amplitude ($\simeq 4s_{24}^2 = 0.1$) is modulated by the $O(1)$ phase $\Delta_{14}^{\text{ND}} = \Delta m_{14}^2 L^{\text{ND}}/4E$. A suppression of this size is certainly allowed by the nuisance parameters of the flux model.⁴ Therefore, for the range of parameters under considerations, the “post-fit” fluxes completely incorporate the 4-flavor effects (if these are present). In this situation, it is problematic to perform an accurate 4-flavor spectral analysis from outside the T2K collaboration, since one would need to model the original fluxes (with their uncertainties) and perform a simultaneous fit of both the ND and the FD event spectra varying the oscillation parameters θ_{24} and Δm_{14}^2 . For these reasons we limit our work to a total rate analysis.

We have checked that in the range of $\Delta m_{14}^2 \in [0.1 - 10] \text{ eV}^2$, the total rate suppression at the ND varies in the range [2, 8]%. For definiteness, in the analysis we assume $\Delta m_{14}^2 = 1 \text{ eV}^2$, for which the total rate suppression is $\sim 4\%$. Consequently, we have increased by the same amount the normalization of the published ν_μ flux. Since the FD total rate is proportional to the product of the non-oscillated flux and the transition probability $P_{\mu e}$, in the fit, a larger flux will be compensated by a lower $P_{\mu e}$. By observing that the leading term of $P_{\mu e}$ is proportional to s_{13}^2 , we can deduce that the estimate of $\sin^2 \theta_{13}$ will be slightly smaller ($\sim -3\%$) with respect to the 3-flavor case, as we have explicitly checked numerically. Therefore, when interpreting the results of the 4-flavor analysis, one should bear in mind that this (small) effect is at play, together with those (larger) described in Sec. II, which are genuine LBL effects.

We remark that the fake energy distortions introduced in the fluxes by the ND280 anchoring procedure are present, basically unaltered, also in the far detector fluxes (which are an extrapolation of the ND fluxes). For this reason, it would be pointless (and wrong) to perform a spectral 4-flavor analysis of the FD data using the published fluxes. As we have shown in the previous subsection on the 3-flavor analysis, the T2K sensitivity is currently dominated by the total rate information. Therefore, it is legitimate to assume that the total rate information will give reliable results also in the 4-flavor analysis, as far as the fake distortions are of the order of a few %. Of course, the situation would be different for values of s_{24}^2 much larger than those considered in this work, in which case a dedicated spectral analysis would be inescapable. The same conclusion would hold if the T2K $\nu_\mu \rightarrow \nu_e$ appearance measurement had considerably larger statistics.

A final remark is in order concerning the treatment of the atmospheric mixing angle θ_{23} . It can be shown that the far/near ratio in the $\nu_\mu \rightarrow \nu_\mu$ channel is almost unaffected by 4-flavor effects, as we have explicitly checked numerically. Therefore, the estimate of θ_{23} is expected to be very stable with respect to the 4-flavor perturbations induced by the small values of s_{24}^2 we are considering. Therefore, in the 4-flavor analysis we have marginalized θ_{23} taking into account the constraint $\sin^2 \theta_{23} = 0.51 \pm 0.05$ obtained, within the 3-flavor framework, from the $\nu_\mu \rightarrow \nu_\mu$ disappearance measurement [33] performed by T2K. This assumption would not be justified for larger values of θ_{24} , in which case the estimate of θ_{23} should be obtained by analyzing the $\nu_\mu \rightarrow \nu_\mu$ disappearance results within a 4-flavor framework.

C. Results of the 3-flavor analysis

In the 3-flavor analysis, the two mixing angles (θ_{13} , θ_{23}) and the CP-phase δ_{13} are treated as free parameters, taking into account the external prior $\sin^2 \theta_{23} = 0.51 \pm 0.05$ provided by the $\nu_\mu \rightarrow \nu_\mu$ disappearance measurement [33] performed by T2K. For the atmospheric mass splitting we use the best fit value $|\Delta m_{13}^2| = 2.4 \times 10^{-3} \text{ eV}^2$ obtained in the same analysis. The solar mass-mixing parameters are fixed at the best fit value obtained in the global analysis [9].

Figure 2 shows the results of the analysis for the two cases of NH (upper panels) and IH (lower panels) in the plane spanned by the two variables $[\sin^2 2\theta_{13}, \delta_{13}]$, the atmospheric mixing angle θ_{23} having been marginalized away. The left panels report the T2K allowed regions for the confidence levels 68% and 90% (1 d.o.f), identical to those used by the T2K collaboration, so as to facilitate comparison. As it can be seen, our results are basically superimposable to those obtained by the collaboration. The thin vertical band displayed in both panels represents the range allowed at 68% C.L. for θ_{13} by the reactor experiments. As already noticed in the global

⁴ Indeed, the ND spectrum normalization appears to be a few % lower than the “pre-fit” one, most of the suppression being concentrated in a region close to the peak of the muon momentum distribution (see Fig. 1 of [2]).

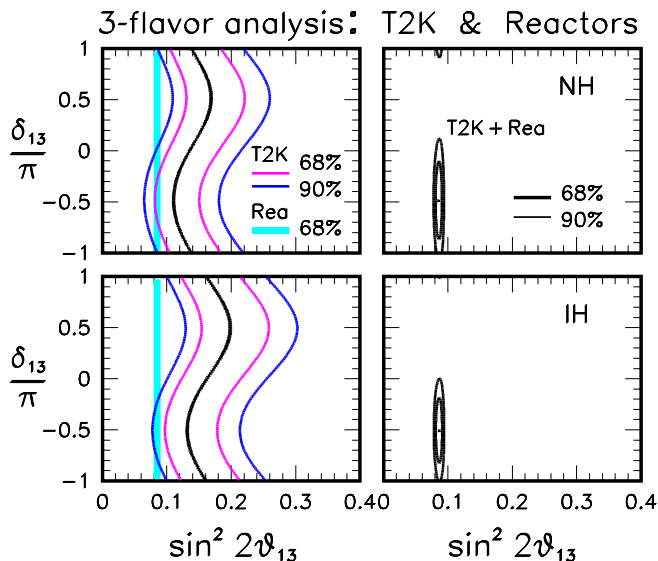


FIG. 2: Left panels: Regions allowed by T2K and by the θ_{13} -sensitive reactor experiments for normal hierarchy (upper panel) and inverted hierarchy (lower panel). Right panels: Region allowed by their combination. The mixing angle θ_{23} is marginalized away. The confidence levels refer to 1 d.o.f. ($\Delta\chi^2 = 1.0, 2.69$).

analyses [9–11] and in partial fits performed by various experimental collaborations, the T2K allowed bands lie at values of θ_{13} , which are somewhat larger compared to the range identified by reactors. As a result, as evident in the two right panels, the combination of the reactor ex-

periments with T2K, tends to select values of $\delta \sim -\pi/2$, disfavoring the case of no CPV ($\delta_{13} = 0, \pi$) at roughly the 90% C.L. In addition, a weak preference for the case of normal hierarchy emerges ($\chi_{\text{NH}}^2 - \chi_{\text{IH}}^2 \simeq -0.8$).

D. Results of the 4-flavor analysis

As discussed in detail in the Appendix, in the 3+1 scheme, the role of matter effects is very similar to the 3-flavor case. Basically (in comparison to the vacuum case), they tend to increase (decrease) the theoretically expected T2K rate in the case of NH (IH), with a consequent downward (upward) shift of the range preferred for θ_{13} . The “wiggles” structure of the allowed regions is basically the same for the two mass hierarchies (see Figs. 3,4). The regions obtained for the case of IH are essentially shifted towards larger values of θ_{13} and slightly expanded with respect to those obtained in the NH case. We describe in detail the results only for NH, the interpretation of the IH case being straightforward.

Figure 3 displays the results of the 4-flavor analysis for the case of NH. The four panels represent the T2K allowed regions in the usual plane [$\sin^2 \theta_{13}, \delta_{13}$] for four different choices of the new CP-phase δ_{14} . We have fixed the four-flavor parameters at the following values: $s_{14}^2 = s_{24}^2 = 0.025$, $s_{34}^2 = 0$, $\delta_{34} = 0$ and $\Delta m_{14}^2 = 1 \text{ eV}^2$. As a benchmark we also report the range allowed for θ_{13} by reactors, which is identical to the standard case. A quick comparison of the four panels of Fig. 3 with the 3-flavor case (left upper panel of Fig. 2) shows the big impact of the 4-flavor effects on the structure of the T2K

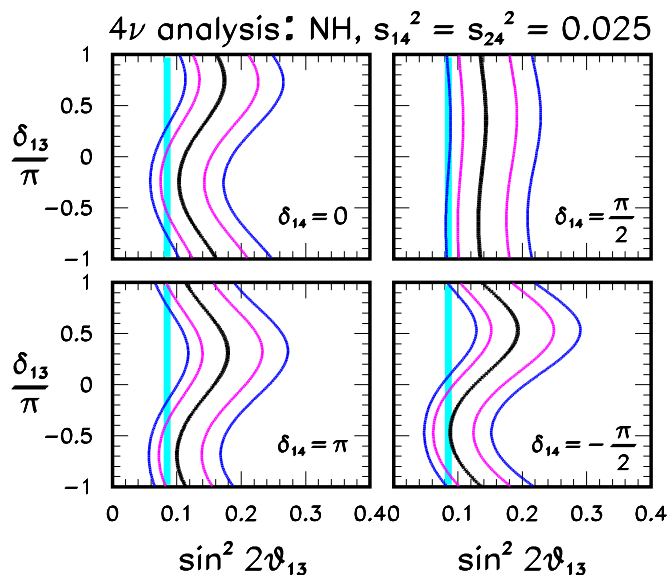


FIG. 3: Regions allowed by T2K for four values of CP-phase δ_{14} . Normal hierarchy is assumed. The mixing angle θ_{23} is marginalized away. The vertical band represents the region allowed by reactor experiments. Confidence levels as in Fig. 2.

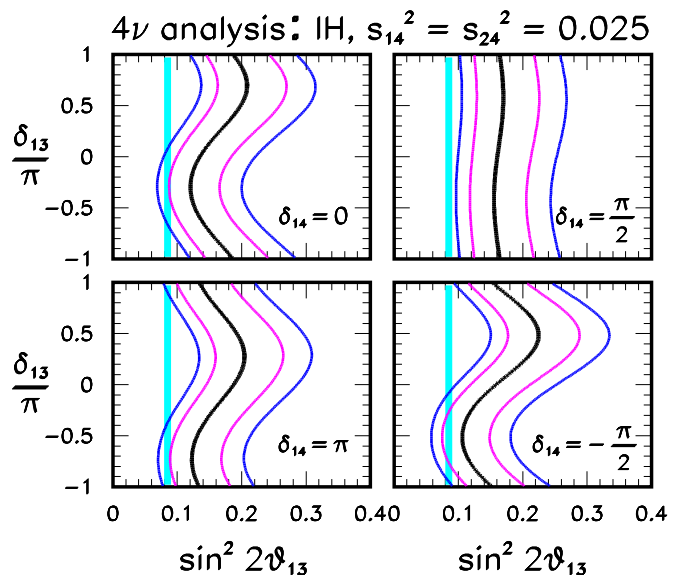


FIG. 4: Regions allowed by T2K for four values of CP-phase δ_{14} . Inverted hierarchy is assumed. The vertical band represents the region allowed by reactor experiments. The mixing angle θ_{23} is marginalized away. Confidence levels as in Fig. 2.

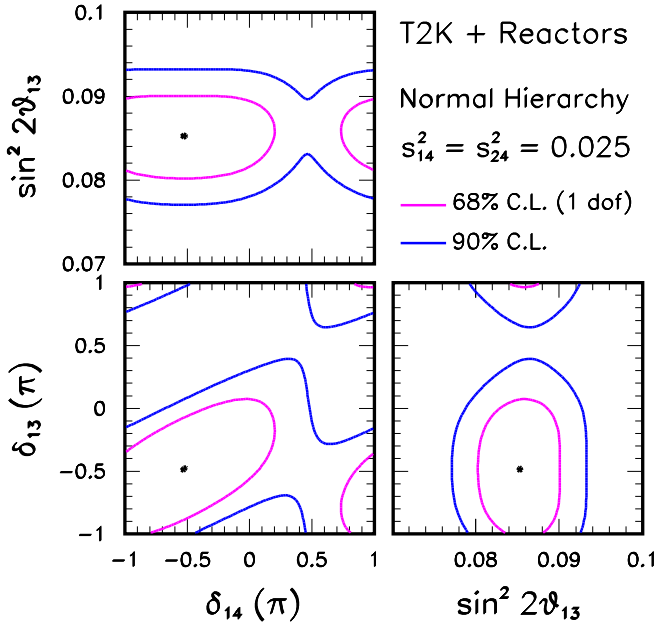


FIG. 5: Regions allowed by the combination of T2K and reactor experiments for the case of normal hierarchy. The mixing angle θ_{23} is marginalized away.

“wiggles”. The behavior of the curves can be easily interpreted, taking into account that the dominant contribution to the total rate comes from a region of the energies close to the first oscillation maximum, where $\Delta \sim \pi/2$. Inspection of Eq. (12) shows that the standard interference term is proportional to $-\sin \delta_{13}$. From Eq. (13) we see that for $\delta_{14} = \pi/2$, the new interference term is proportional to $\sin \delta_{13}$. Therefore, in this case the two terms are in opposition of phase and having similar amplitudes their sum will tend to cancel out, making the “wiggles” almost to disappear (right upper panel). In this case, the T2K region is basically a vertical band.

For $\delta_{14} = -\pi/2$ (right lower panel) the two interference terms have the same phase and the horizontal excursion of the “wiggles” is increased (roughly doubled). As a benchmark, the best-fit curve excursion range is $[0.11, 0.17]$ in the 3-flavor case, while it is $[0.9 - 0.19]$ in the 4-flavor one. In the two cases $\delta_{14} = 0, \pi$ (left panels) the new interference term is proportional to $\pm \cos \delta_{13} = \pm \sin(\pi/2 - \delta_{13})$ and thus it has a $\pm\pi/2$ difference of phase with respect to the standard one. As a result, in such two cases, the behavior of the T2K bands is intermediate between the two cases $\delta_{14} = (-\pi/2, \pi/2)$ described above and shown in the two right panels.

It is interesting to note that, in the presence of 4-flavor effects, a better agreement among the estimates of θ_{13} from reactors and T2K can be obtained. In particular, this occurs for $\delta_{14} \simeq -\pi/2$, which is therefore expected to be the best fit value in the combined analysis of reactors with T2K. We recall that (a small) part of the shift towards lower values of θ_{13} of the T2K bands is imputable to the re-normalization of the non-oscillated ν_μ

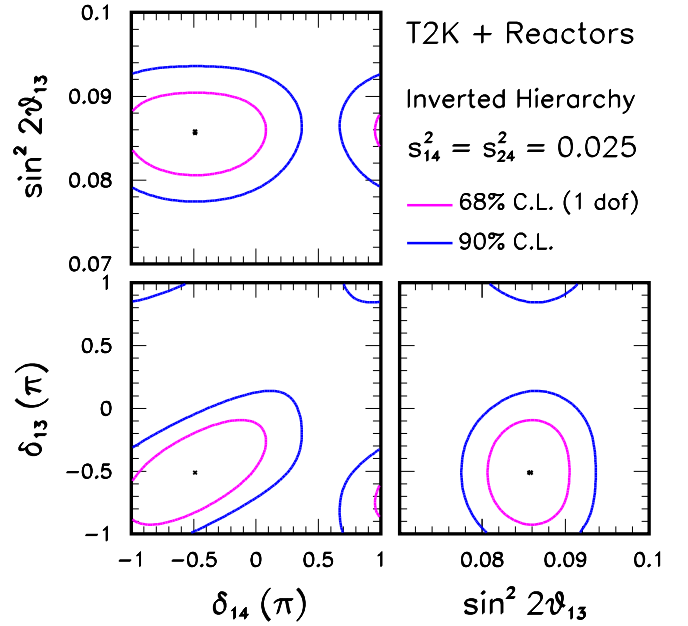


FIG. 6: Regions allowed by the combination of T2K and reactor experiments for the case of inverted hierarchy. The mixing angle θ_{23} is marginalized away.

flux, which we have incorporated in our analysis in order to take into account the effect of the oscillations at the near detector ND280 (see the discussion in subsection III.A.2).

As a last step in our 4-flavor analysis, we perform the combination of T2K with reactors. In this more general analysis, we treat the two mixing angles (θ_{13}, θ_{23}) and the two CP-phases (δ_{13}, δ_{14}) as free parameters, while fixing the remaining 4-flavor parameters at the same values used before: $s_{14}^2 = s_{24}^2 = 0.025$, $s_{34}^2 = 0$, $\delta_{34} = 0$ and $\Delta m_{14}^2 = 1 \text{ eV}^2$. We have checked that the impact of non-zero θ_{34} (and consequently of the associated CP-phase δ_{34}) is negligible, even considering very large values of θ_{34} , well beyond the current bounds. The insensitivity to θ_{34} in vacuum is obvious from the formulae presented in Sec. II. The reason of its irrelevance also in matter is explained in the Appendix.

Similarly to the 3-flavor case, in the T2K + Reactor combination, the (CP-phases independent) estimate of θ_{13} provided by the reactor experiments selects those subregions of the T2K bands which have a statistically significant overlap with such an estimate. These, in turn, correspond to allowed regions in the plane $[\delta_{13}, \delta_{14}]$ spanned by the two CP-phases. Figures 5 and 6 display such regions for the two cases of NH and IH, together with the 2-dimensional projections having as one of the two variables the mixing angle θ_{13} . As expected a preference for values of $\delta_{13} \sim \delta_{14} \sim -\pi/2$ emerges. The absence of CP violation is disfavored at a slightly lower confidence level in comparison with the 3-flavor case. This is imputable to the bigger freedom allowed by the larger parameter space available in the 3+1 scheme.

IV. CONCLUSIONS AND OUTLOOK

We have investigated the impact of light (eV) sterile neutrinos in the long-baseline experiment T2K. We have shown that, within the 3+1 scheme, for mass-mixing parameters suggested by the short-baseline anomalies, the new term appearing in the $\nu_\mu \rightarrow \nu_e$ transition probability arising from the interference between the sterile and the atmospheric oscillation frequencies, has the same order of magnitude of the standard 3-flavor solar-atmospheric interference term. As a result, the current T2K data (in combination with the θ_{13} -dedicated reactor experiments) are sensitive to two of the three CP-violating phases involved in the 3+1 scheme. In particular, we found that both the standard phase and the new one ($\delta_{13} \equiv \delta$ and δ_{14} in our parameterization choice) tend to have a common best fit value $\delta_{13} \simeq \delta_{14} \sim -\pi/2$. In addition, quite intriguingly, our analysis shows that the inclusion of sterile neutrino effects leads to a better agreement of the estimate of θ_{13} obtained from reactors with that extracted from T2K, which (in the 3-flavor framework) tends to be larger than the first one.

Our results make it evident that T2K and other similar LBL experiments (like MINOS and NO ν A in the near future) should be routinely included in the global fits involving sterile neutrinos. We finally stress that, in the eventuality of a discovery of light sterile neutrino species at the upcoming SBL experiments, our findings would represent the first information on the sterile-induced CPV sources. The LBL accelerator experiments already operational and those planned for the future (LBNE, LBNO and T2HK) will play a key role in extracting more information on the new CPV sector, whose exploration has just begun.

Appendix: Treatment of the MSW effect

The Hamiltonian in the flavor basis can be written as

$$H = UKU^\dagger + V, \quad (20)$$

where K denotes the diagonal matrix containing the wavenumbers $k_i = m_i^2/2E$ ($i = 1, 2, 3, 4$) (m_i^2 and E being the neutrino squared-mass and energy respectively), while the matrix V incorporates the position-independent matter MSW potential [34, 35]. Barring irrelevant factors proportional to the identity, we can define the diagonal matrix containing the three relevant wavenumbers as

$$K = \text{diag}(0, k_{12}, k_{13}, k_{14}), \quad (21)$$

and the matrix encoding the matter effects, as

$$V = \text{diag}(V_{CC}, 0, 0, -V_{NC}), \quad (22)$$

where

$$V_{CC} = \sqrt{2}G_F N_e \quad (23)$$

is the charged-current interaction potential of the electron neutrinos with the background electrons having number density N_e , and

$$V_{NC} = -\frac{1}{2}\sqrt{2}G_F N_n \quad (24)$$

is the neutral-current interaction potential (common to all the active neutrino species) with the background neutrons having number density N_n . For later convenience, we also introduce the positive-definite ratio

$$r = -\frac{V_{NC}}{V_{CC}} = \frac{1}{2} \frac{N_n}{N_e}, \quad (25)$$

which in the earth is approximately $r \simeq 0.5$. In order to simplify the treatment of matter effects in LBL experiments it is useful to introduce a new basis

$$\bar{\nu} = \bar{U}^\dagger \nu, \quad (26)$$

where

$$\bar{U} = \tilde{R}_{34} R_{24} \tilde{R}_{14} \quad (27)$$

is the part of the mixing matrix defined in Eq. (1) containing only the rotations involving the fourth neutrino mass state. In this new basis, the Hamiltonian assumes the form

$$\bar{H} = \bar{H}^{\text{kin}} + \bar{H}^{\text{dyn}} = U_{3\nu} K U_{3\nu}^\dagger + \bar{U}^\dagger V \bar{U}, \quad (28)$$

where the first term is the kinematic contribution describing the oscillations in vacuum, and the second one represents a non-standard dynamical term. Since $|k_{14}|$ is much bigger than k_{12} and $|k_{13}|$ and much bigger than one, we can reduce the dynamics to that of an effective 3-flavor system. Indeed, from Eq. (28) one has that the (4,4) entry of \bar{H} is much bigger than all the other elements and, at the leading order, (the absolute value of) the fourth eigenvalue of \bar{H} is much larger than the other three ones. As a result, the state $\bar{\nu}_s$ evolves independently of the others. Extracting from \bar{H} the submatrix with indices (1, 2, 3), one obtains the 3×3 Hamiltonian

$$\bar{H}_{3\nu} = \bar{H}_{3\nu}^{\text{kin}} + \bar{H}_{3\nu}^{\text{dyn}}, \quad (29)$$

governing the evolution of the $(\bar{\nu}_e, \bar{\nu}_\mu, \bar{\nu}_\tau)$ system, whose dynamical part has the form

$$\bar{H}^{\text{dyn}} = V_{CC} \begin{pmatrix} |\bar{U}_{e1}|^2 + r|\bar{U}_{s1}|^2 & r\bar{U}_{s1}^* \bar{U}_{s2} & r\bar{U}_{s1}^* \bar{U}_{s3} \\ \dagger & r|\bar{U}_{s2}|^2 & r\bar{U}_{s2}^* \bar{U}_{s3} \\ \dagger & \dagger & r|\bar{U}_{s3}|^2 \end{pmatrix}, \quad (30)$$

where, for brevity, we have indicated with \dagger the complex conjugate of the matrix element having the same two indexes inverted. In deriving Eq. (30) we have made use of the relations $\bar{U}_{e2} = \bar{U}_{e3} = \bar{U}_{\mu 3} = 0$. Considering the explicit expressions of the elements of \bar{U} , Eq. (30) takes the form

$$\bar{H}^{\text{dyn}} = V_{CC} \begin{pmatrix} c_{14}^2 + r c_{34}^2 c_{24}^2 s_{14}^2 & r c_{34}^2 c_{24} s_{14} s_{24} & r c_{34} c_{24} s_{14} s_{34}^* \\ \dagger & r c_{34}^2 s_{24}^2 & r c_{34} s_{24} s_{34}^* \\ \dagger & \dagger & r s_{34}^2 \end{pmatrix} \quad (31)$$

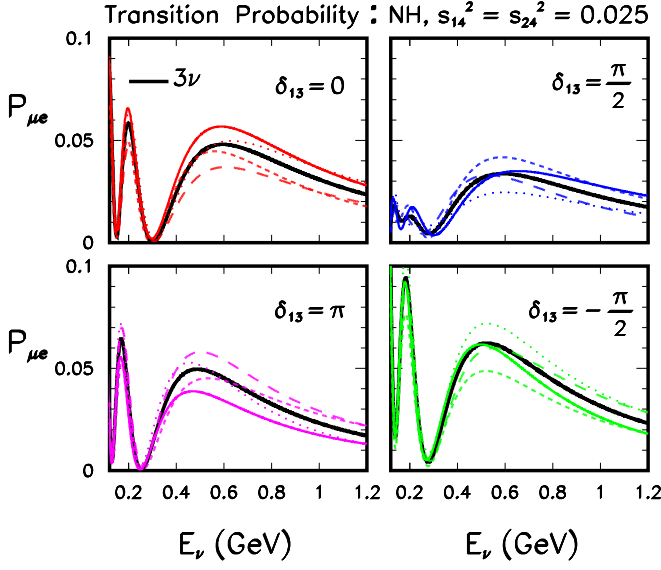


FIG. 7: Probability of $\nu_\mu \rightarrow \nu_e$ transition in the 3+1 scheme. The four panels correspond to four different values of the standard CP-phase δ_{13} . In each panel, the black thick solid line represents the 3-flavor case ($\theta_{14} = \theta_{24} = 0$), while the colored lines represent the 4-flavor case (with $s_{14}^2 = s_{24}^2 = 0.025$) for the following four different values of the non-standard CP-phase: $\delta_{14} = 0$ (solid), $\delta_{14} = \pi$ (long-dashed), $\delta_{14} = \pi/2$ (short-dashed), $\delta_{14} = -\pi/2$ (dotted).

which, for vanishing sterile neutrino angles ($\theta_{14} = \theta_{24} = \theta_{34} = 0$) returns the standard 3-flavor MSW potential. For small values of such mixing angles, the dynamical term is approximated by

$$\bar{H}^{\text{dyn}} \approx V_{\text{CC}} \begin{pmatrix} 1 - (1-r)s_{14}^2 & r\bar{s}_{14}s_{24} & r\bar{s}_{14}\bar{s}_{34}^* \\ \dagger & rs_{24}^2 & rs_{24}s_{34}^* \\ \dagger & \dagger & rs_{34}^2 \end{pmatrix}. \quad (32)$$

This shows that the corrections to the standard potential are of the second order⁵ in the new s_{ij} 's and further suppressed by a factor r or $(1-r)$, in the earth being $r \sim 0.5$. Therefore, for realistic values of the mixing angles, these corrections are $O(\epsilon^2)$, and hence at the level of a few %. Taking into account that in T2K also the *standard* matter effects are small being $v = V_{\text{CC}}/|k_{13}| \sim 0.05$, the new non-standard effects have amplitudes of a few ‰ and have a completely negligible impact. We have numerically checked that allowing for very large values of θ_{34} (which is the least known of the three new mixing angles) even beyond the range currently allowed by the global fits, the transition probability is indistinguishable from the case of $\theta_{34} = 0$. Therefore, the independence of the transition probability from θ_{34} , which is exact in vacuum, remains essentially valid also in the presence of matter

⁵ A similar behavior has been observed to occur for solar neutrino transitions induced by sterile species [36].

effects. For this reason, the results of the analysis presented in the previous section, albeit formally obtained for the fixed value $\theta_{34} = 0$, are indeed more general, being equivalent to those one would obtain by treating θ_{34} and δ_{34} as free parameters and marginalizing over them.

For the calculation of the transition probability, it is useful to define the evolution operator, which, in the rotated basis, takes the form

$$\bar{S} \equiv e^{-i\bar{H}L} \approx \begin{pmatrix} e^{-i\bar{H}_{3\nu}L} & \mathbf{0} \\ \mathbf{0} & e^{-ik_{14}L} \end{pmatrix}, \quad (33)$$

and is connected to the evolution operator in the original flavor basis through the unitary transformation

$$S = \bar{U}\bar{S}\bar{U}^\dagger. \quad (34)$$

Taking into account the block-diagonal form of \bar{S} and the relations $\bar{U}_{e2} = \bar{U}_{e3} = \bar{U}_{\mu3} = 0$, one has for the relevant transition amplitude

$$S_{e\mu} = \bar{U}_{e1} [\bar{U}_{\mu1}^* \bar{S}_{ee} + \bar{U}_{\mu2}^* \bar{S}_{e\mu}] + \bar{U}_{e4} \bar{U}_{\mu4}^* \bar{S}_{ss}. \quad (35)$$

Since $\bar{S}_{ss} = e^{-ik_{14}L}$ oscillates very fast, the associated terms are averaged out by the finite energy resolution of the detector, and for the transition probability we have

$$P_{\mu e}^{4\nu} \equiv |S_{e\mu}|^2 = |\bar{U}_{\mu1}|^2 |\bar{U}_{e1}|^2 |\bar{S}_{ee}|^2 + |\bar{U}_{\mu2}|^2 |\bar{U}_{e1}|^2 |\bar{S}_{e\mu}|^2 + 2|\bar{U}_{e1}|^2 \text{Re}[\bar{U}_{\mu1}^* \bar{U}_{\mu2} \bar{S}_{ee} \bar{S}_{e\mu}^*] + |\bar{U}_{e4}|^2 |\bar{U}_{\mu4}|^2. \quad (36)$$

This expression is completely general, except for the assumption of averaged oscillations, and connects the 4-flavor transition probability to the amplitudes and probabilities of the effective 3-flavor system governed by the effective Hamiltonian in Eq. (29). Considering the explicit expressions of the elements of the matrix \bar{U} , Eq. (36) becomes

$$P_{\mu e}^{4\nu} = s_{24}^2 s_{14}^2 c_{14}^2 \bar{P}_{ee}^{3\nu} + c_{24}^2 c_{14}^2 \bar{P}_{\mu e}^{3\nu} - 2c_{14}^2 c_{24} s_{14} s_{24} \text{Re}(e^{-i\delta_{14}} \bar{S}_{ee} \bar{S}_{e\mu}^*) + s_{14}^2 s_{24}^2 c_{14}^2, \quad (37)$$

where $\bar{P}_{ee}^{3\nu} \equiv |\bar{S}_{ee}|^2$ and $\bar{P}_{\mu e}^{3\nu} \equiv |\bar{S}_{e\mu}|^2$. Therefore, the 4-flavor problem is reduced to a more familiar 3-flavor case, for which one needs to calculate the elements \bar{S}_{ee} and $\bar{S}_{e\mu}$. Figure 7 displays some selected numerical examples of the 4-flavor probabilities calculated using Eq. (37). The four panels correspond to four different values of the standard CP-phase δ_{13} . In each panel, the black thick solid line represents the 3-flavor case ($\theta_{14} = \theta_{24} = 0$), while the colored lines represent the 4-flavor case (with $s_{14}^2 = s_{24}^2 = 0.025$) for the following four different values of the non-standard CP-phase: $\delta_{14} = 0$ (solid), $\delta_{14} = \pi$ (long-dashed), $\delta_{14} = \pi/2$ (short-dashed), $\delta_{14} = -\pi/2$ (dotted).

While the 3-flavor elements \bar{S}_{ee} and $\bar{S}_{e\mu}$ can be evaluated numerically (as we have done) approximate expressions already existing in the literature in various limits may help to further simplify the expression of the transition probability in Eq. (37), which, for small values of the two mixing angles θ_{14} and θ_{24} , takes the form

$$P_{\mu e}^{4\nu} \simeq (1 - s_{14}^2 - s_{24}^2) \bar{P}_{\mu e}^{3\nu} - 2s_{14}s_{24} \text{Re}(e^{-i\delta_{14}} \bar{S}_{ee} \bar{S}_{e\mu}^*) + s_{14}^2 s_{24}^2 (1 + \bar{P}_{ee}^{3\nu}). \quad (38)$$

First of all it can be noted that for small values of $s_{13} \sim \epsilon$ and $\alpha\Delta \sim \epsilon^2$ one has [37]

$$\bar{S}_{ee} \simeq 1 - O(\epsilon^2). \quad (39)$$

Since we are interested to terms up to $O(\epsilon^4)$, we can assume $\bar{S}_{ee} = 1$. Moreover, for small (standard) matter effects, the 3-flavor amplitude $\bar{S}_{e\mu}$ has the well known (see for example [37]) form

$$\bar{S}_{e\mu} \simeq A s_{13}^m \sin \Delta^m + B(\alpha\Delta), \quad (40)$$

where A and B are two complex coefficients with $O(1)$ modulus, given by

$$A = -2i s_{23} e^{-i(\Delta + \delta_{13})}, \quad (41)$$

$$B = -2i c_{23} s_{12} c_{12}, \quad (42)$$

where (s_{13}^m, Δ^m) are the approximated expressions of (θ_{13}, Δ) in matter

$$s_{13}^m \simeq (1 + v) s_{13}, \quad (43)$$

$$\Delta^m \simeq (1 - v) \Delta, \quad (44)$$

with $v = V_{CC}/|k_{13}| \simeq 0.05$. Including Eqs. (39-42) in the expression of the transition probability in Eq. (38), in the limit case $v = 0$ we recover, in an alternative way, the fourth order expansion of the vacuum formula in Eq. (13) presented in Sec. II. For $v \neq 0$, one sees that the structure of the transition probability remains the same as in vacuum, containing six terms of which three are of the interference type. The only impact of matter effects (at least for the T2K setup) is to break the degeneracy among NH and IH, exactly as it occurs in the 3-flavor case, because of the shifts $s_{13} \rightarrow s_{13}^m$ and $\Delta \rightarrow \Delta^m$ in Eqs. (43,44).

Acknowledgments

A. P. acknowledges support from the European Community through a Marie Curie IntraEuropean Fellowship, grant agreement no. PIEF-GA-2011-299582, ‘‘On the Trails of New Neutrino Properties’’. We acknowledge partial support from the European Union FP7 ITN Invisibles (Marie Curie Actions, PITN-GA-2011-289442).

-
- [1] N. Cabibbo, Phys. Lett. B **72**, 333 (1978).
[2] K. Abe *et al.* [T2K Collaboration], Phys. Rev. Lett. **112**, 061802 (2014) [arXiv:1311.4750 [hep-ex]].
[3] P. Adamson *et al.* [MINOS Collaboration], Phys. Rev. Lett. **112**, 191801 (2014) [arXiv:1403.0867 [hep-ex]].
[4] C. Zhang [Daya Bay Collaboration] Talk given at the XXVI International Conference on Neutrino Physics and Astrophysics, Boston, USA, June 2-7, 2014.
[5] F. P. An *et al.* [Daya Bay Collaboration], Phys. Rev. Lett. **112**, 061801 (2014) [arXiv:1310.6732 [hep-ex]].
[6] Y. Abe *et al.* [Double Chooz Collaboration], JHEP **1410**, 86 (2014) [arXiv:1406.7763 [hep-ex]].
[7] S.-H. Seo [RENO Collaboration] Talk given at the XXVI International Conference on Neutrino Physics and Astrophysics, Boston, USA, June 2-7, 2014, [arXiv:1410.7987 [hep-ex]].
[8] Y. Suzuki [for the Super-Kamiokande Collaboration], Talk given at the NIAPP Topical Workshop, Munich Institute for Astro- and Particle Physics, 10 July 2014.
[9] F. Capozzi, G. L. Fogli, E. Lisi, A. Marrone, D. Montanino and A. Palazzo, Phys. Rev. D **89** (2014) 093018 [arXiv:1312.2878 [hep-ph]].
[10] M. C. Gonzalez-Garcia, M. Maltoni and T. Schwetz, JHEP **1411**, 052 (2014) [arXiv:1409.5439 [hep-ph]].
[11] D. V. Forero, M. Tortola and J. W. F. Valle, Phys. Rev. D **90**, 093006 (2014) [arXiv:1405.7540 [hep-ph]].
[12] A. Palazzo, Mod. Phys. Lett. A **28**, 1330004 (2013) [arXiv:1302.1102 [hep-ph]].
[13] J. Kopp, P. A. N. Machado, M. Maltoni and T. Schwetz, JHEP **1305**, 050 (2013) [arXiv:1303.3011 [hep-ph]].
[14] C. Giunti, M. Laveder, Y. F. Li and H. W. Long, Phys. Rev. D **88**, 073008 (2013) [arXiv:1308.5288 [hep-ph]].
[15] A. Donini and D. Meloni, Eur. Phys. J. C **22**, 179 (2001) [hep-ph/0105089].
[16] A. Donini, M. Lusignoli and D. Meloni, Nucl. Phys. B **624**, 405 (2002) [hep-ph/0107231].
[17] A. Donini, M. Maltoni, D. Meloni, P. Migliozzi and F. Terranova, JHEP **0712** (2007) 013 [arXiv:0704.0388 [hep-ph]].
[18] A. Dighe and S. Ray, Phys. Rev. D **76**, 113001 (2007) [arXiv:0709.0383 [hep-ph]].
[19] A. Donini, K. i. Fuki, J. Lopez-Pavon, D. Meloni and O. Yasuda, JHEP **0908**, 041 (2009) [arXiv:0812.3703 [hep-ph]].
[20] O. Yasuda, arXiv:1004.2388 [hep-ph].
[21] D. Meloni, J. Tang and W. Winter, Phys. Rev. D **82**, 093008 (2010) [arXiv:1007.2419 [hep-ph]].
[22] B. Bhattacharya, A. M. Thalappilil and C. E. M. Wagner, Phys. Rev. D **85**, 073004 (2012) [arXiv:1111.4225 [hep-ph]].
[23] A. Donini, P. Hernandez, J. Lopez-Pavon, M. Maltoni and T. Schwetz, JHEP **1207**, 161 (2012) [arXiv:1205.5230 [hep-ph]].
[24] D. Hollander and I. Mocioiu, arXiv:1408.1749 [hep-ph].
[25] J. Schechter, J. W. F. Valle, Phys. Rev. D **22**, 2227 (1980).
[26] K. Nakamura *et al.* (Particle Data Group), J. Phys. G **37**, 075021 (2010).

- [27] C. Jarlskog, Phys. Rev. Lett. **55**, 1039 (1985).
- [28] A. Cervera, A. Donini, M. B. Gavela, J. J. Gomez Cadenas, P. Hernandez, O. Mena and S. Rigolin, Nucl. Phys. B **579**, 17 (2000) [Erratum-ibid. B **593**, 731 (2001)] [hep-ph/0002108].
- [29] K. Asano and H. Minakata, JHEP **1106**, 022 (2011) [arXiv:1103.4387 [hep-ph]].
- [30] A. Palazzo, JHEP **1310**, 172 (2013) [arXiv:1308.5880 [hep-ph]].
- [31] K. Abe *et al.* [T2K Collaboration], Phys. Rev. D **87**, 012001 (2013) [arXiv:1211.0469 [hep-ex]].
[32]
- [32] <http://t2k-experiment.org/results/neutrino-beam-flux-2013/>
- [33] K. Abe *et al.* [T2K Collaboration], Phys. Rev. Lett. **112**, no. 18, 181801 (2014) [arXiv:1403.1532 [hep-ex]].
- [34] L. Wolfenstein, Phys. Rev. D **17**, 2369 (1978).
- [35] S. P. Mikheev and A. Yu. Smirnov, Yad. Fiz. **42**, 1441 (1985) [Sov. J. Nucl. Phys. **42**, 913 (1985)].
- [36] A. Palazzo, Phys. Rev. D **83**, 113013 (2011) [arXiv:1105.1705 [hep-ph]].
- [37] T. Kikuchi, H. Minakata and S. Uchinami, JHEP **0903**, 114 (2009) [arXiv:0809.3312 [hep-ph]].